1999PASJ...51..445S

PASJ: Publ. Astron. Soc. Japan **51**, 445–448 (1999)

Dark Bulge, Exponential Disk, and Massive Halo in the Large Magellanic Cloud

Yoshiaki SOFUE
Institute of Astronomy, University of Tokyo, Mitaka, Tokyo 181-8588
E-mail: sofue@ioa.s.u-tokyo.ac.jp

(Received 1999 May 17; accepted 1999 June 10)

Abstract

The rotation curve of the Large Magellanic Cloud, which we derived from high-resolution H I position-velocity diagrams observed by Kim et al. (1998 ApJ 503, 674), shows a steep central rise and flat rotation with a gradual rise toward the edge. Using the rotation curve, we calculate the distribution of the surface mass density, and show that the LMC has a dark compact bulge, an exponential disk, and a massive halo. The bulge is 1.2 kpc away from the center of the stellar bar, and is not associated with an optical counterpart. This indicates that the "dark bulge" has a large fraction of dark matter, with an anomalously high mass-to-luminosity (M/L) ratio. On the contrary, the stellar bar has a smaller M/L ratio compared to that of the surrounding regions.

Key words: Dark matter — Magellanic Clouds — Mass distribution — Rotation

1. Introduction

The rotation curves of dwarf galaxies are known to increase monotonically toward their outer edge; the mass-to-luminosity ratio, and therefore the dark-matter fraction, is larger than that in usual spiral galaxies (Persic et al. 1996). However, little is known about their internal distribution of dynamical mass, because of insufficient spatial resolution due to their small angular extents as well as the low surface brightness in the H I and Hα lines.

H I observations of the Large Magellanic Cloud (LMC), the nearest dwarf galaxy, have provided us with a unique opportunity to study detailed kinematics (e.g., Luks, Rohlfs 1992; Putman et al. 1998). Recently, Kim et al. (1998) obtained high-resolution H I kinematics from interferometer observations. They have shown that the rotation characteristics is nearly axisymmetric; this fact allows us to derive a reliable rotation curve by using a position-velocity diagram along the major axis.

In the present paper, we derive a new rotation curve for the LMC, and discuss the distribution of dynamical mass and dark matter.

2. Position-Velocity Diagrams and Rotation Curve

Figure 1 shows the H I velocity field as reproduced from Kim et al. (1998), superposed on a smoothed DSS (Digitized Sky Survey) image in the B band. The cross indicates the kinematical center defined by Kim et al. We have, here, determined the position, RA=5 h 13.8 m, Dec = $-68°38'$ (J2000), as indicated by the asterisk, at which the velocity gradient attains its maximum value, and around which the velocity field becomes most symmetric. From the symmetric velocity field, we may assume that the gas is circularly rotating around this kinematical center in the central 2-kpc radius region. The interferometer observations may miss the intensities from an extended gas disk. However, since the extended gas and the gaseous features detected with the interferometer are thought to be rotating at the same speed, we assume that the observed velocity field represents that of the total gas.

In figure 2 we reproduce the PV diagram across a position close to the adopted kinematical center from Kim et al. (1998). The thin line represents a rotation curve fitted by Kim et al. using an AIPS utility, which adopts a simple function. However, the innermost part of the PV diagram shows a much steeper variation from positive to negative velocities, which appears to be not well traced. In order to obtain a more precise rotation velocities in the innermost region, we applied the envelope-tracing method of maximum-velocities (Sofue 1996). The newly determined rotation velocities are indicated by the thick curve, by which the steep velocity variation is now well traced. Besides the bright features traced by this curve, a higher velocity feature is found at -60 to -70 km s^{-1} and $+20'$. If we trace this feature, the velocity variation around the center becomes steeper, and the rotation curve will have a much steeper rise at the center.

Using the thick curve in figure 2 and correcting for an inclination angle of 33°, we obtained the rotation curve

© Astronomical Society of Japan • Provided by the NASA Astrophysics Data System

1999PASJ...51..445S

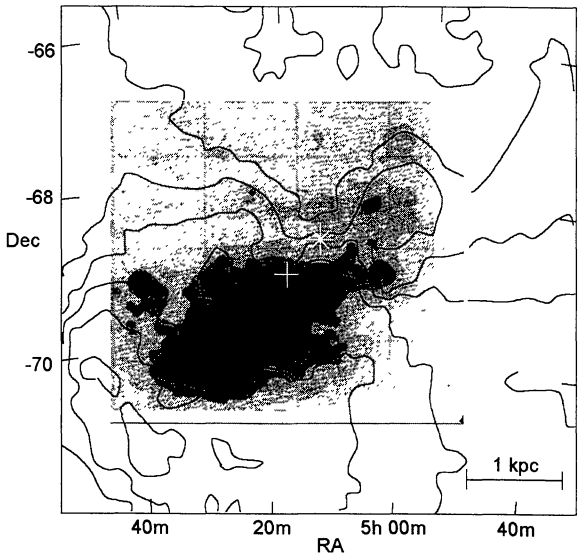

Fig. 1. HI velocity field of LMC (Kim et al. 1998) superposed on a smoothed DSS image in the B band. The cross indicates the kinematical center of Kim et al. (1998), and the asterisk is the adopted center position in this paper. Note the significant displacement of the bar from the kinematical center.

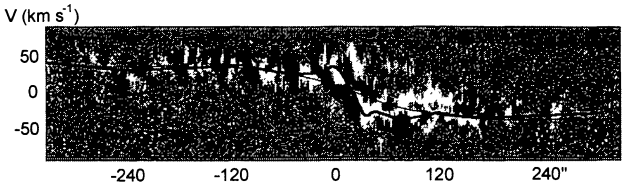

Fig. 2. Position-velocity diagram of the LMC along the major axis (Kim et al. 1998). We traced the maximum-velocity envelope by the thick line to derive the rotation curve.

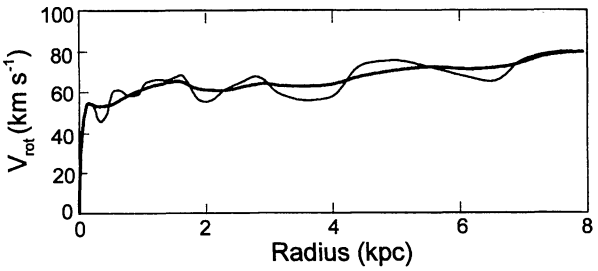

Fig. 3. Rotation curve of the LMC. Note the steep central rise and flat disk rotation. The thin line denotes the observation, and the thick line is a smoothed rotation curve, which we adopted to calculate the surface-mass distribution.

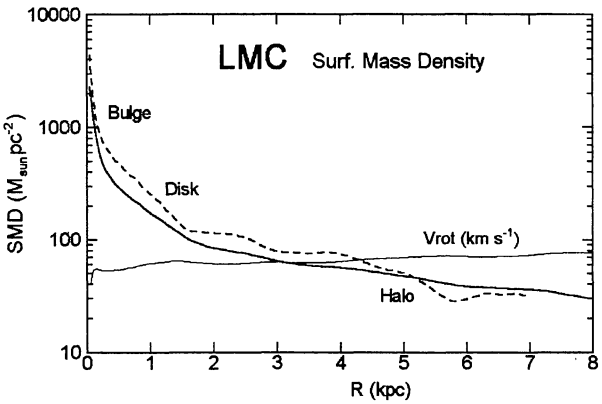

Fig. 4. Radial distributions of the surface mass density for a thin-disk assumption (full line) and for a spherical assumption (dashed line). There appear to be three components: (1) a dense and compact bulge at radii < 240 pc, (2) an exponential disk until 2 to 3 kpc, and (3) a massive halo.

as shown in figure 3. The outer rotation curve beyond the HI disk up to 8 kpc was taken from Kunkel et al. (1997). In the following discussion, we adopt the thick curve in figure 3, which was drawn by smoothing the observed curve (thin line). The thus-obtained rotation curve is found to be similar to those of the usual disk galaxies (Rubin et al. 1982; Sofue 1996, 1997; Sofue et al. 1998, 1999) except for the absolute values. The rotation curve of the LMC is characterized as follows:

(1) a steep central rise,
(2) a flat part in the disk, and
(3) a gradual rise toward the edge.

3. Surface Mass Distribution: Bulge, Disk, and Massive Halo

Given a rotation curve from the center to the outer edge with a sufficient resolution, we can directly calculate the surface mass density (SMD)(Takamiya, Sofue 1999). This method is not intervened by any models, such as the Plummer potentials and exponential disks. An extreme case is to assume spherical symmetry; the rotation velocity is used to calculate the total mass involved within a radius, which is then used to calculate the SMD. Another extreme case is to assume a thin rotating disk: the SMD can be directly calculated by using the Poisson equation. We assumed that the true mass distribution could lie in between these two cases, which were indeed found to coincide within a factor of 1.5. Figure 4 shows the calculated

© Astronomical Society of Japan • Provided by the NASA Astrophysics Data System

1999PASJ...51..445S

SMD for the disk (full line) and spherical cases (dashed line). The full line should better represent a disk component, as the H I appearance indicates, while the spherical case would be better for an inner bulge. The obtained SMD distribution can be summarized as in the following.

3.1. Dark Bulge

The distribution of SMD shows a compact, high-density component tightly concentrated around the kinematical center. Because this component is not associated with an optical counterpart, we call it a "dark bulge". The e-folding scale radius is about 120 pc when fitted with an exponential function. The mass involved within 240 pc radius, at which the SMD becomes equal to that of the disk component, is $\sim 1.7 \times 10^8\,M_\odot$. Except for its small radius, the dark bulge is as dense as the central bulge of normal disk galaxies; the SMD is estimated to be $\sim 1.0 \times 10^3\,M_\odot$ pc^{-2} at its scale radius, which is comparable to or only by a factor of ten smaller than the values of the usual galactic bulges ($\sim 10^{3-4}\,M_\odot$ pc^{-2}) at their scale radii (a few hundred pc) (Takamiya, Sofue 1999).

3.2. Exponential Disk

The SMD, then, is followed by an exponentially decreasing part with an e-folding scale radius of 1.0 kpc. This "exponential disk" in mass is dominant up to a radius of 2 kpc, and extends to 3 to 4 kpc radius, being gradually replaced by an extended halo component. The total mass involved within 2 kpc radius is $\sim 2 \times 10^9\,M_\odot$, consistent with the value obtained by Kim et al. (1998). The SMD of $\sim 200\,M_\odot$pc^{-2} at its scale radius is comparable to the values of the usual disk galaxies ($\sim$ 300–500 $M_\odot$pc^{-2}) at their scale radii ($\sim$ 3–5 kpc). The total B magnitude of LMC is 0.6 mag. within an angular extent of $650' \times 550'$, or within ~ 4.3 kpc radius (de Vaucouleurs et al. 1991). For a distance modulus of 18.50 (50 kpc) and $B-V$ color of 0.55, we obtain a V magnitude of -18.45. This leads to a V band luminosity of $\sim 2 \times 10^9\,L_\odot$. Since the mass involved within 4.3 kpc is $\sim 4.5 \times 10^9\,M_\odot$, we obtain a mean M/L ratio of about 2.2 for the disk component.

3.3. Massive Halo

The SMD in the outer halo obeys an exponentially decreasing function with an e-folding scale radius of 5.2 kpc. The total mass involved within 8 kpc radius is $\sim 1 \times 10^{10}\,M_\odot$. The fact that the outer envelope is not visible in optical photographs (DSS) suggests again a high M/L ratio in the halo. This is consistent with the high M/L ratio in many other dwarf galaxies, for which gradually rising rotation curves are generally observed (Persic et al. 1996). Kunkel et al. (1997) have suggested that the high velocities in the outer region could be due to a tidal effect with the Small Magellanic Cloud. Alternatively, tidal warping could also cause apparently higher (or lower) velocities, because the galaxy is nearly face on. In these cases, the presently estimated mass would be significantly overestimated.

4. Discussion

The dark bulge is significantly displaced from the stellar bar. No optical counterpart is visible, despite the idea that the extinction is supposed to be not large for the nearly face-on orientation. Since the surface luminosity appears to be not significantly enhanced from the average in the disk part, where the M/L ratio is ~ 2, the bulge's M/L would be as large as $\sim$ 20–50 $M_\odot/L_\odot$. Such a high M/L indicates a significant excess of the dark-matter fraction in the bulge. As discussed in section 2, if the faint and higher-velocity features in the PV diagrams are taken into account, the rotation curve would have a much steeper rise in the center than that traced by the thick line in figure 2. If this is the case, the bulge's mass density could still be higher, as is the dark mass fraction.

The center of the stellar bar is about 1.2 kpc away from the center of the dark bulge (figure 1). No significant mass enhancement, which might be related to the bar, can be detected at radii 1 to 2 kpc in figure 4. In fact, neither a stream motion in the velocity field, nor any anomaly in the PV diagrams are observed along the stellar bar (Kim et al. 1998). We may argue that the M/L ratio in the stellar bar is significantly lower than that in the surrounding regions.

We finally comment on an alternative possibility to explain the displacement of the optical and kinematical centers. Ram-pressure stripping of the gas disk either due to an intergalactic wind (Sofue 1994) and/or a gaseous inflow from the Small Magellanic Cloud (Gardiner et al. 1994; Putman et al. 1998) could cause such a displacement. In order for the H I velocity field being kept unperturbed, it must occur as quickly as in the crossing time of the innermost disk, or within $t \sim r/v_{\rm rot} \sim 2 \times 10^6$ yr, where $r \sim 120$ pc is the radius of the innermost H I disk and $v_{\rm rot} \sim 55$ km s^{-1} is the rotating velocity. This requires a wind velocity greater than $v_{\rm ram} \sim d/t \sim 500$ km s^{-1}, where $d \sim 1$ kpc is the displacement. Such a high velocity would be possible for an intergalactic wind. However, the ram-stripping condition, $\rho_{\rm ram} v_{\rm ram}^2 > \rho_{\rm HI} v_{\rm rot}^2$, seems not to be satisfied: for $\rho_{\rm ram} \sim 10^{-4} m_{\rm H}$ cm^{-3}, $v_{\rm ram} \sim 500$ km s^{-1}, $\rho_{\rm HI} \sim 0.1\ m_{\rm H}$ cm^{-3}, and $v_{\rm rot} \sim 55$ km s^{-1}, we have 0.5×10^{-12} and 5×10^{-12} dyne cm^{-2} for the first and second terms, respectively. Therefore, ram-stripping does not appear to be a likely origin. In any other circumstances, where no gravitational attraction is present, the inner-rotation feature could disappear within about one million years. Thus, in so far as the velocity field is as-

© Astronomical Society of Japan • Provided by the NASA Astrophysics Data System

1999PASJ...51..445S

sumed to represent rotation, a high-density mass concentration at the kinematical center, and therefore the presence of a dark bulge, could be an inevitable consequence.

Another possible idea is to attribute the velocity gradients in the kinematical center to local velocity anomalies, such as that due to wiggles by H I shells and/or turbulence. However, Kim et al.'s modulus map of velocity residuals indicates that density waves and warping are more dominant to cause the residuals. Neither the largest H I shells nor 30 Dor are associated with the largest velocity residuals and wiggles. Moreover, there appear no particular H I shells or associated star-forming regions around the kinematical center where the velocity variation is steepest.

Hence, we here rely more on our assumption that the H I kinematics of the LMC directly manifests the dynamics of the galaxy. We also comment that, if we adopt the smooth rotation curve of Kim et al. (1998) as an alternative case, the mass distribution would be similar to the one represented by the disk component in figure 4. Even in this case the mass center is still significantly displaced from the optical bar, and no particular optical enhancement corresponding to the exponential disk is recognized around the kinematical center.

The author thanks T. Takamiya for calculating the SMD from the rotation curve data. He is also indebted to Prof. M. Fujimoto of Nagoya University for invaluable discussions.

References

de Vaucouleurs G., de Vaucouleurs A., Corwin H.G. Jr, Buta R.J., Paturel G., Fouqué P. 1991, in Third Reference Catalogue of Bright Galaxies (Springer Verlag, New York)
Gardiner L.T., Sawa T., Fujimoto M. 1994, MNRAS 266, 567
Kim S., Stavely-Smith L., Dopita M.A., Freeman K.C., Sault R.J., Kesteven M.J., McConnell D. 1998, ApJ 503, 674
Kunkel W.E., Demers S., Irwin M.J., Albert L. 1997, ApJ 488, L129
Luks Th., Rohlfs K. 1982, A&A 263, L41
Persic M., Salucci P., Stel F. 1996, MNRAS 281, 27
Putman M.E., Gibson B.K., Staveley-Smith L., Banks C., Barnes D.G. et al. 1998, Nature 394, 752
Rubin V.C., Ford W.K., Thonnard N., Burstein D. 1982, ApJ 261, 439
Sofue Y. 1994, PASJ 46, 431
Sofue Y. 1996, ApJ 458, 120
Sofue Y. 1997, PASJ 49, 17
Sofue Y., Tomita A., Honma M.,Tutui Y., Takeda Y. 1998, PASJ 50, 427
Sofue Y., Tutui Y., Honma M., Tomita A., Takamiya T., Koda J., Takeda Y. 1999, ApJ in press
Takamiya T., Sofue Y. 1999, ApJ submitted

© Astronomical Society of Japan • Provided by the NASA Astrophysics Data System